Physics of Fluids

Experimental study of particle electrophoresis in shear-thinning fluids

Cite as: Phys. Fluids **31**, 022002 (2019); https://doi.org/10.1063/1.5085186
Submitted: 10 December 2018 . Accepted: 08 January 2019 . Published Online: 01 February 2019

Amirreza Malekanfard, Chien-Hsuan Ko (柯建亘), Di Li (李迪), Logan Bulloch, Alicia Baldwin, Yao-Nan Wang (王耀男), Lung-Ming Fu (傅龍明), and Xiangchun Xuan (宣向春)

Physics of Fluids ARTICLE scitation.org/journal/phf

Experimental study of particle electrophoresis in shear-thinning fluids

Cite as: Phys. Fluids 31, 022002 (2019); doi: 10.1063/1.5085186
Submitted: 10 December 2018 • Accepted: 8 January 2019 •
Published Online: 1 February 2019

Amirreza Malekanfard,[1] Chien-Hsuan Ko (柯建亘),[1,2] Di Li (李迪),[1] Logan Bulloch,[1] Alicia Baldwin,[1] Yao-Nan Wang (王耀男),[3] Lung-Ming Fu (傅龍明),[4] and Xiangchun Xuan (宣向春)[1,a)]

AFFILIATIONS

[1]Department of Mechanical Engineering, Clemson University, Clemson, South Carolina 29634-0921, USA
[2]Graduate Institute of Materials Engineering, National Pingtung University of Science and Technology, Pingtung, Taiwan
[3]Department of Vehicle Engineering, National Pingtung University of Science and Technology, Pingtung 912, Taiwan
[4]Department of Engineering Science, National Cheng Kung University, Tainan 701, Taiwan

[a)]**Author to whom correspondence should be addressed:** xcxuan@clemson.edu. **Tel.:** 864-656-5630. **Fax:** 864-656-7299.

ABSTRACT

Electric field is the method of choice in microfluidic devices for precise transport and placement of particles via fluid electroosmosis and particle electrophoresis. However, current studies on particle electrophoresis in microchannels have been focused mainly upon Newtonian fluids though many of the chemical and biological fluids possess non-Newtonian characteristics. Especially lacking is the experimental study of particle electrophoresis in either type of fluids. We report in this work an unprecedented experimental observation that polystyrene particles migrate towards the walls of straight rectangular microchannels in the electroosmotic flow of shear-thinning xanthan gum (XG) solutions. This phenomenon is opposite to the particle focusing along the channel center in our control experiment with the Newtonian base fluid of the XG solutions. It is attributed to a fluid shear thinning-induced lift that overcomes the wall-induced repulsive electrical lift. The parametric effects of the fluid-particle-channel-(electric) field system are systematically investigated.

I. INTRODUCTION

Microfluidic devices have been increasingly used over the past two decades for numerous chemical, biomedical, and environmental applications because of the advantages (e.g., reduced cost, increased efficiency, and portability) over their macroscopic counterparts.[1,2] A precise transport and placement (e.g., focusing, trapping, and sorting) of particles (from biological to synthetic, soft to rigid, etc.) in microchannels is often involved in these devices.[3–6] Among the various particle handling approaches (e.g., optical, acoustic, and magnetic),[7–10] electric field is the method of choice in microfluidic systems because of the ease of operation and integration (with pre- and/or post-analysis parts).[11–16] It controls the motion of particles by fluid electroosmosis and particle electrophoresis, both of which are linear electrokinetic phenomena and result from the Coulomb force acting on the net charge inside the electric double layer (EDL) formed at the fluid-solid (i.e., the channel walls and particles) interface.[17] Under the limit of thin EDLs, electroosmotic flow owns a plug-like velocity profile and has a similitude to the electric field in Newtonian fluids. Electric field, if non-uniform in, for example, straight microchannels with varying cross-sections[18–20] or curved microchannels[21–23], also generates particle dielectrophoresis, which is a nonlinear electrokinetic phenomenon either along or against its gradients.[24,25]

There have been quite a number of studies on particle electrophoresis in Newtonian fluids through straight microchannels of various shapes (e.g., cylindrical, slit, and rectangular channels, where electric field is uniform everywhere, and hence, dielectrophoresis is absent).[26,27] These studies have been primarily concerned about two aspects. One aspect is the wall effect on the axial electrophoretic motion of particles, which has been theoretically and experimentally

demonstrated to reduce the particle velocity[28–32] unless particles travel in close proximity to channel walls.[33–36] The other aspect is the wall-induced lateral migration of particles,[37,38] which is driven by the repulsive electrical lift because of the mismatched fluid and particle conductivities.[39–42] Recently, there have been a few studies on the cross-stream particle migration in combined electric field- and pressure-driven fluid flows, where particles are observed to migrate towards either the center or the walls of straight microchannels depending on the direction of electric field.[43–45] Particles have also been reported to self-assemble into near-wall periodic bands in countercurrent electroosmotic and Poiseuille flows though the mechanism is currently still unclear.[46,47]

As many of the chemical (e.g., polymer solutions) and biological (e.g., DNA solutions) samples are complex fluids,[48,49] there has been a growing interest in the understanding of non-Newtonian effects (e.g., elasticity and shear thinning) on particle electrophoresis (as well as fluid electroosmosis[50–54]) in microchannels.[55] However, the majority of these studies are purely theoretical or numerical, which predict an enhanced electrophoretic velocity of particles in Carreau fluids as compared to Newtonian fluids in various confinements (e.g., spherical cavity and cylindrical channel) because of the fluid shear thinning effect.[56–59] In another theoretical study, particles are found to exhibit a shape- and size-dependent electrophoretic velocity in complex fluids with shear rate dependent viscosities.[60]

Thus far, there have been very few experimental works on particle electrophoresis or fluid electroosmosis in non-Newtonian fluids. Instabilities have been reported to occur in the electroosmotic flow of polyacrylamide (PAA) solutions, which have strong elasticity and shear thinning effects, through both a constriction[61] and a cross-shaped microchannel.[62] They also take place in xanthan gum (XG) solutions,[63] which are strongly shear thinning with a weak elasticity.[64,65] Recently, our group has observed unexpected oscillations of particles traveling along with the electroosmotic flow of polyethylene oxide (PEO) solutions, which are moderately elastic and weakly shear thinning, through a constriction microchannel.[66] Such oscillations within the constriction were later found to disappear for particles traveling against the flow.[67] More recently, our group has demonstrated an exactly opposite lateral migration of particles in a combined electric field- and pressure-driven flow of PEO solution as compared to that in a Newtonian fluid.[68]

We present in this work an experimental study of particle electrophoresis in XG solutions through straight rectangular microchannels. We find that particles migrate towards the channel walls, which is exactly opposite to the particle focusing phenomenon along the channel center in Newtonian fluids.[69] We perform a comprehensive study of various parameters of the fluid-particle-channel-(electric) field system that may potentially affect such an unprecedented particle migration phenomenon in non-Newtonian fluids.

II. EXPERIMENT

A. Microchannel fabrication

The microchannel used in this work was fabricated using polydimethylsiloxane (PDMS) with the standard soft lithography technique. The geometry of the channel was designed in AutoCAD (Autodesk, Inc.), and printed onto a transparent film at a high resolution (10 000 DPI, CAD/Art Services, Inc.) for uses as a negative photomask. In order to make microchannels with different depths, negative photoresist (SU-8 25, MicroChem Corp.) was coated (WS-400E-NPP-Lite, Laurell Technologies) onto thoroughly cleaned glass slides at different spin speeds. A two-step soft bake (the baking temperature and time depend on the thickness of the spin-coated photoresist film) was then performed on two separate hot plates (Torrey Pines Scientific) for each photoresist-covered slide. Following that was a UV exposure (ABM, Inc.) upon the photoresist through the same negative photomask while the exposure time varied with the film thickness. After another two-step post-exposure bake, the cross-linked photoresist was soaked in a developer solution (MicroChem Corp.) and rinsed using isopropyl alcohol (Fisher Scientific). This step created a positive replica of the microchannel on the glass slide, which, after a final hard bake, was ready for uses as a mold.

Next, liquid PDMS (Dow Corning Corp., Midland, USA) was prepared by thoroughly mixing Sylgard 184 and its curing agent (Dow Corning) at a 10:1 ratio in weight. It was then poured over the microchannel mold in a petri dish followed by a degassing process in a vacuum oven (13-262-280A, Fisher Scientific). Subsequently, the petri dish was placed into a gravity convection oven (13-246-506GA, Fisher Scientific) to cure the liquid PDMS at 70 °C for 2 h. After that, the PDMS section containing the channel was cut out using a scalpel, and two through holes were punched in the pre-designed circular regions at the channel ends as reservoirs. The last step of the whole fabrication process was to plasma-treat (PDC-32G, Harrick Scientific) the channel side of the PDMS slab (around 3 mm thick) and a clean glass slide before bonding them together. Figure 1 shows a picture of the microchannel, which is straight 2 cm long with a rectangular cross-section. The width of the channel was fixed at 50 μm in this work while the depth was varied from 15 μm to 25 μm and 40 μm.

B. Particle solutions preparation

Polystyrene spheres (Sigma-Aldrich Corp.) of 5 μm, 10 μm, and 15 μm in diameter were used to study particle electrophoresis in the fabricated rectangular microchannels. They were each re-suspended in 2000 ppm XG solution that was prepared by dissolving XG powder (Tokyo Chemical Industry) into 1 mM phosphate buffer (pH $\approx$ 7.4 with a measured electric conductivity of 200 μS/cm). Moreover, 10 μm particles were re-suspended into 1 mM phosphate buffer-based 1000 ppm and 3000 ppm XG solutions for the study of XG concentration effect. They were also re-suspended into the pure 1 mM buffer solution for a control experiment. All three types

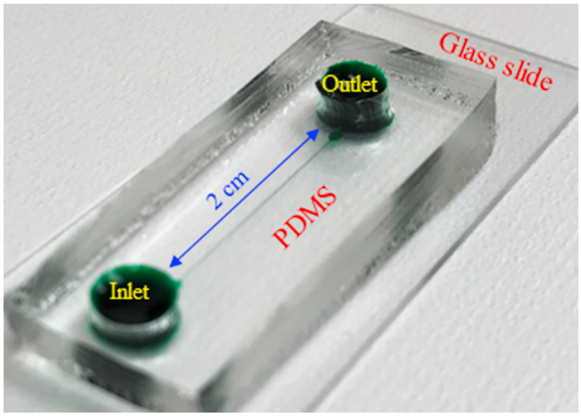

FIG. 1. Picture of the microfluidic chip where the straight rectangular microchannel is located at the bottom surface of the PDMS slab and sealed with a glass slide.

of particles reached a final concentration of 10^6–10^7 particles/ml in every suspension. To reduce particle aggregations and adhesions (to microchannel walls), 0.5% (in volume ratio) Tween 20 (Fisher Scientific) was added into each particle solution. Table I summarizes the rheological properties of the prepared XG and buffer solutions, which are directly adapted from the literature[70] due to the lack of measuring equipment in our lab. The fluid shear-thinning effect is reflected by the power-law index, n, where the Newtonian buffer solution has $n = 1$ while the XG solutions are all strongly shear thinning with $n < 0.5$. Moreover, the XG solution becomes more shear thinning at a higher concentration.

C. Experimental method

To generate electric field across the length of the microchannel, one platinum electrode (Fisher Scientific) was inserted into each of the solution-filled reservoirs at the channel ends. Different magnitudes of direct current (DC) voltage were supplied using a high-voltage power supply (Glassman High Voltage, Inc.). The electric field was kept no more than 400 V/cm in any test to minimize potential Joule heating effects.[71] Prior to every test, the liquid height was carefully balanced in the two reservoirs to eliminate pressure-driven flow in the microchannel. Moreover, the running time of electric field was limited to 1 min to minimize the electroosmosis-induced pressure-driven backflow.[72] Each test was repeated a minimum of three times on different days to make sure that results were repeatable. The visualization and recording of particle motion were done through an inverted microscope (Nikon Eclipse TE2000U; Nikon Instruments) equipped with a CCD camera (Nikon DS-Qi1Mc). The obtained digital images were post-processed using Nikon imaging software (NIS-Elements AR 2.30). The ImageJ software package (National Institute of Health) was employed to measure the transverse particle positions at the channel outlet, which were then used to calculate the probability distribution function (PDF) for Excel plots.

TABLE I. Rheological properties (zero shear viscosity, η_0; infinite shear viscosity, η_∞; power-law index, n) of the prepared suspending fluids at 20 °C.

Solutions	η_0 (Pa s)	η_∞ (Pa s)	n
1 mM buffer	1.0×10^{-3}	1.0×10^{-3}	1.0
1000 ppm XG	0.225	1.88×10^{-3}	0.40
2000 ppm XG	3.68	2.24×10^{-3}	0.34
3000 ppm XG	120	3.91×10^{-3}	0.23

Particles were observed to move against the electric field direction in all three XG solutions. Their axial velocities at different transverse positions were obtained using the particle tracking velocimetry (i.e., particle's travelling distance divided by the time span of measurement) near the channel inlet (still 4 mm away from the entrance to ensure a fully developed flow and a uniform electric field). The electrokinetic mobility of particles, μ_{EK}, was then determined from the slope of the linear trendline of the experimentally determined particle velocities (averaged over at least five individual particles) vs. electric field. This operation was based on the assumption that the electrokinetic particle velocity is proportional to the electric field magnitude,[55–59] which is supposed reasonable because the fluid velocity is very low in all our tests and hence yields insignificant shear thinning effect.

III. RESULTS AND DISCUSSION

A. Development of particle migration along the channel length

Figure 2(a) shows the top-view images of 10 μm particles in 2000 ppm XG solution through a 25 μm deep microchannel under a 150 V/cm DC electric field. For a better illustration of the development of particle electrophoresis, six images were obtained capturing the inlet, four middle segments and outlet, respectively, along the channel length. Each of these images, which shows the particle streaklines over an approximately 200 μm channel length, was taken roughly 3.8 mm away from the previous one making them evenly distributed along the entire channel (2 cm long). One can observe in Fig. 2(a) that particles tend to move more towards the walls of the microchannel as they move through it. This trend is also quantitatively illustrated by the plots of particle PDF in Fig. 2(b), where more than 85% of the flowing particles are within one particle diameter from the walls at the channel outlet. Such a wall-directed lateral particle migration in the XG solution is opposite to that in the Newtonian buffer solution, where, as demonstrated in Fig. 2(c), particles are focused to a single stream along the channel center at the outlet. The latter phenomenon is a consequence of the wall-induced electrical lift, F_w, which results from the dissimilar electric conductivities of the particles and suspending fluid,[37–39]

$$F_w \sim \varepsilon a^2 E^2 \tag{1}$$

In this equation, ε is the fluid permittivity, a is the particle diameter, and E is the applied electric field. Note that F_w is

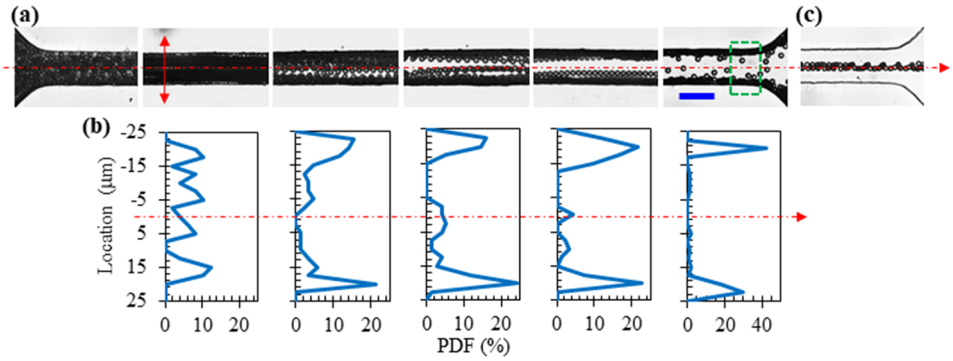

FIG. 2. Electrophoresis of 10 μm particles through a 25 μm deep straight rectangular microchannel under 150 V/cm DC electric field: (a) top-view superimposed images in 2000 ppm XG solution at selected channel segments; (b) plots of particle PDF in 2000 ppm XG solution at the selected channel segments except the inlet; (c) top-view superimposed image in the Newtonian buffer solution at the channel outlet. The dashed box in (a) highlights the region where the particle PDF was obtained. The solid-line arrow in (a) indicates the vertical axis of the particle PDF plots in (b). The dashed-dotted lines in (a) and (b) both indicate the channel centerline. The scale bar in (a) represents 50 μm.

a strong function of the particle-wall distance and becomes zero at the center of the channel.[69]

As the dielectrophoretic-like force,[39] F_w, is supposed to also take place in the non-Newtonian XG solution, we hypothesize there exists another lateral force in the shear-thinning XG solution that directs particles towards the channel walls and competes with F_w. This force should not be an elastic-like lift, F_{eL}, which, as traditionally defined for fluids with a negligible second normal stress difference (N_2), is proportional to the variation of the first normal stress difference, N_1, over the size of the particle.[73] By assuming a power-law behavior, $N_1 = A\dot{\gamma}^m$, for diluted solutions of high molecular weight polymers,[74] we obtain

$$F_{eL} \sim a^3 A \nabla \dot{\gamma}^m \tag{2}$$

where A and m are both fluid-dependent constants with m typically in the range $1 < m \leq 2$, and $\dot{\gamma}$ is the local fluid shear rate. As the electroosmotic velocity profile of shear thinning fluids is uniform under the thin EDL limit (the estimated Debye length is on the order of 10 nm in 1 mM solution,[17] much smaller than the dimension of microchannels or particles in our test), the value of $\dot{\gamma}$ becomes essentially zero everywhere leading to $F_{eL} = 0$. Therefore, we further speculate that the additional wall-directed lateral force arise from the shear thinning effect of the XG solution itself. The mechanism behind this force, F_{ST}, is, however, currently unclear. We present in the following sections a parametric study of the factors that may potentially affect the lateral particle migration in the electroosmotic flow of XG solutions through straight rectangular microchannels.

B. Effect of electric field

Figure 3 shows the effect of electric field magnitude on the lateral migration of 10 μm particle electrophoresis in 2000 ppm XG solution through a 25 μm deep straight microchannel. At 50 V/cm, all particles are observed from the top-view superimposed image in Fig. 3(a) to line the walls at the channel outlet. At 100 V/cm, a very small portion of the particles moves slightly away from the channel walls. Specifically, the PDF plot in Fig. 3(b) shows that more than 95% of the particles are still within one particle diameter from the walls at 100 V/cm. This value drops to around 85% at 150 V/cm [see Fig. 2(c)] and 70% at 200 V/cm [see Fig. 3(b)] because particles increasingly move away from the channel walls. With the further increase of electric field to 300 V/cm

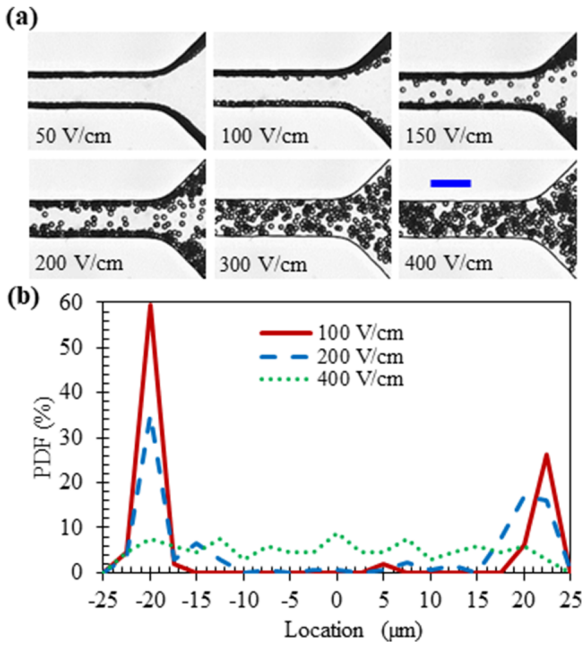

FIG. 3. Electrophoresis of 10 μm particles in 2000 ppm XG solution through a 25 μm deep microchannel under varying DC electric fields: (a) top-view superimposed images at the channel outlet; (b) plot of particle PDF obtained from the images in (a) under three representative electric fields. The scale bar in (a) represents 50 μm.

and above, no apparent particle migration towards the walls is viewed from the images in Fig. 3(a). The PDF plot in Fig. 3(b) presents a nearly even distribution of particles over the channel width at the electric field of 400 V/cm. Such a trend in particle distribution indicates that the above assumed fluid shear-thinning induced lift, F_{ST}, might be insensitive to the applied electric field or has a weaker dependence on electric field than that of the wall-induced electrical lift, F_w.

Figure 4 shows the effect of electric field magnitude on the measured axial electrokinetic velocity of 10 μm particles in 2000 ppm XG solution through a 25 μm deep microchannel. To obtain the particle velocity profile over the channel cross-section, we divided the 50 μm channel width into four equal sections of 12.5 μm each, i.e., two sections each in half channel width. We measured the velocities of (minimum) five particles in every section at a channel segment 4 mm away from the channel inlet [see Fig. 2(a)] and used their average as the electrokinetic velocity therein. Figure 4(a) shows the widthwise distribution of this measured particle velocity under 150 and 300 V/cm electric fields, respectively. A nearly flat profile is obtained for each field, which seems consistent with the plug-like electroosmotic fluid velocity under the thin EDL limit.[55] Figure 4(b) shows the variation of electrokinetic particle velocity with electric field, which is fitted well to a linear trendline with R^2 = 0.9567. The slope of this trendline gives the electrokinetic mobility of 10 μm particles in 2000 ppm XG solution, which was found to be 1.96×10^{-8} $m^2/(V\ s)$ as displayed in Fig. 4(b).

C. Effect of XG concentration

Figure 5 shows the effect of XG concentration on the lateral migration of 10 μm particle electrophoresis in a 25 μm deep straight microchannel. As seen from the top-view images at the channel outlet in Fig. 5(a), particles apparently migrate towards the channel walls in 1000 ppm XG solution under a 100 V/cm electric field. The extent of migration is, however, much smaller than that in 2000 ppm XG solution under the same electric field. It does not change significantly when the XG concentration is further increased to 3000 ppm. This trend verifies our assumption of fluid shear-thinning induced lift, F_{ST}, in XG solutions, which, by nature, should increase for a higher XG concentration. Under a 200 V/cm electric field, particles become roughly uniformly distributed in 1000 ppm XG solution while majority of the particles still remain close to the channel walls in 2000 ppm and 3000 ppm XG solutions. This phenomenon is quantitatively demonstrated by the PDF plot in Fig. 5(b), where the curves for the two higher XG

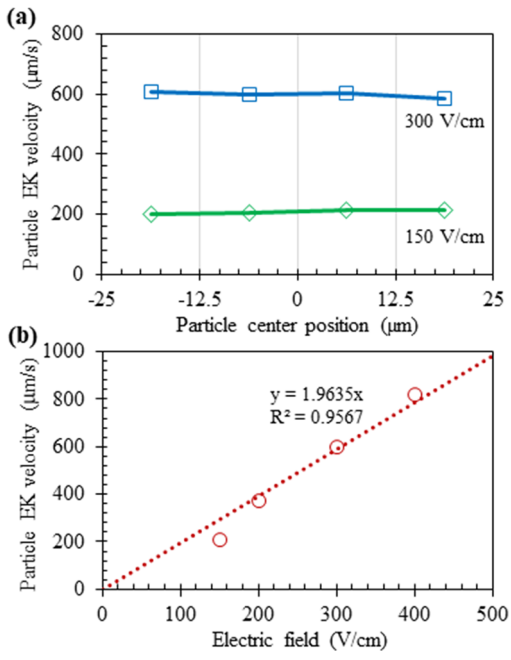

FIG. 4. Experimentally measured axial electrokinetic velocity of 10 μm particles in 2000 ppm XG solution through a 25 μm deep microchannel: (a) velocity profiles in the channel width direction under 150 V/cm and 300 V/cm DC electric fields (symbols represent the experimental data; the solid lines are for guiding the eyes only); (b) velocity variation with electric field (symbols represent the experimental data; the dotted line is the linear trendline of the experimental data with the equation and R^2 values being both displayed).

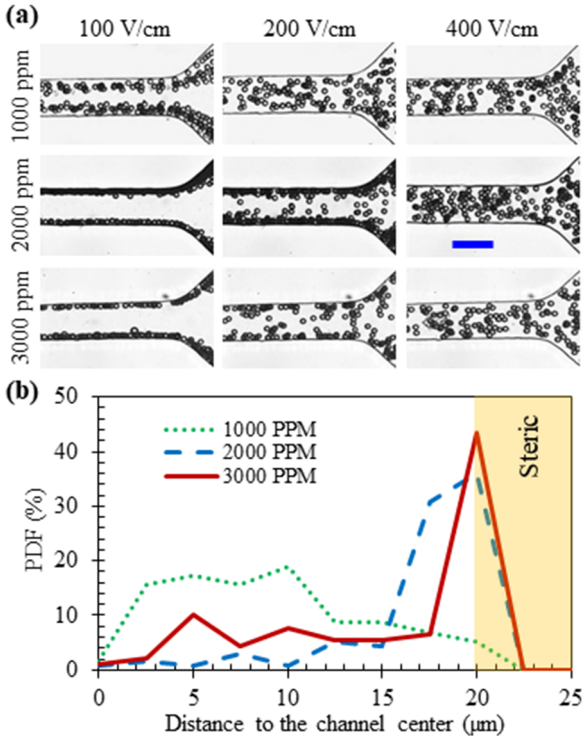

FIG. 5. Electrophoresis of 10 μm particles in XG solutions of varying concentrations through a 25 μm deep microchannel: (a) top-view superimposed images at the channel outlet under varying DC electric fields; (b) plot of particle PDF obtained from the images in (a) under a fixed electric field of 200 V/cm. The scale bar in (a) represents 50 μm. The shaded region in (b) highlights the steric zone adjacent to any channel walls where the center of particles cannot reach.

concentrations are visually comparable. Note that the horizontal axis of the PDF plot in Fig. 5(b) uses the distance of particles to the channel center, and hence, the vertical axis gives the total PDF value for particles of equal distance to either channel wall. At the electric field of 400 V/cm, particles become dispersed across the channel width in all three XG concentrations [see Fig. 5(a)] due to the stronger dependence of the wall-repulsive electrical lift, F_w, on electric field magnitude.

D. Effect of particle size

Figure 6 shows the effect of particle size on the lateral migration of particle electrophoresis in 2000 ppm XG solution through a 25 μm deep microchannel. Under a 100 V/cm electric field, particles of 10 and 15 μm diameters all travel out of the channel lining its two walls as illustrated by the top-view images in Fig. 6(a). In contrast, there is still a small portion of 5 μm particles scattered in the bulk at the channel outlet. This discrepancy, however, does not necessarily mean the wall-directed lateral migration due to fluid shear thinning increases for larger particles because there are far more 5 μm particles in the suspension than the other two sizes. Such a judgement is further supported by the particle images at 200 V/cm in Fig. 6(a), where a good amount of particles of each size stays close to the walls at the channel outlet despite the enhancement in the wall-induced electrical lift, F_w. The PDF plots of the three types of particles are not significantly different in Fig. 6(b) if we take into consideration the steric effect of particle size (see the shaded region for 5 μm particles). Specifically, the center of rigid spherical particles of any sizes cannot approach within one particle radius from any channel walls. In fact, due to the strong size-dependence of the wall-repulsive electrical lift, F_w [see Eq. (1)], the percentage of particles within one particle diameter from either channel walls decreases from 75% for 5 μm particles to around 70% and 55% for 10 and 15 μm particles, respectively. We therefore speculate that the fluid shear-thinning induced lift, F_{ST}, may be simply a linear function of particle size.

E. Effect of microchannel depth

Figure 7 shows the effect of microchannel depth on 10 μm particle electrophoresis in 2000 ppm XG solution under varying DC electric fields. At 100 V/cm, particles migrate towards the walls and travel along them at the outlet in all

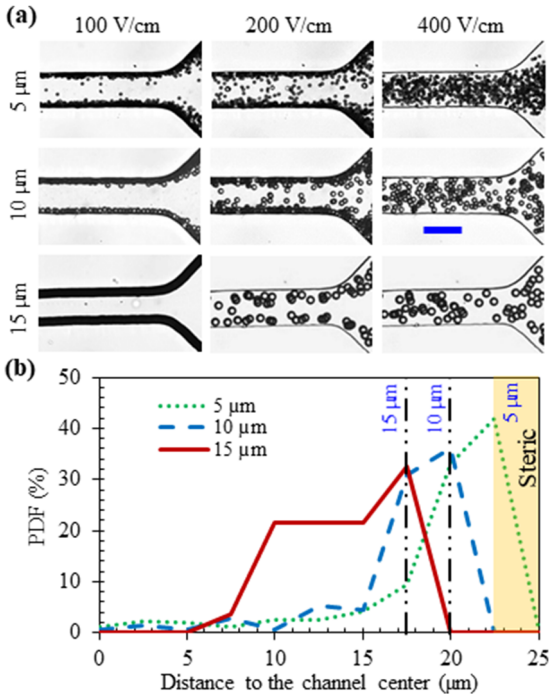

FIG. 6. Electrophoresis of 5 μm, 10 μm, and 15 μm particles in 2000 ppm XG solution through a 25 μm deep microchannel: (a) top-view superimposed images at the channel outlet under varying DC electric fields; (b) plot of particle PDF obtained from the images in (a) under the electric field of 200 V/cm. The scale bar in (a) represents 50 μm. The shaded region in (b) highlights the steric zone adjacent to any channel walls, where the center of 5 μm particles cannot reach. The two vertical dashed-dotted lines highlight the edges of steric zone for 10 μm and 15 μm particles.

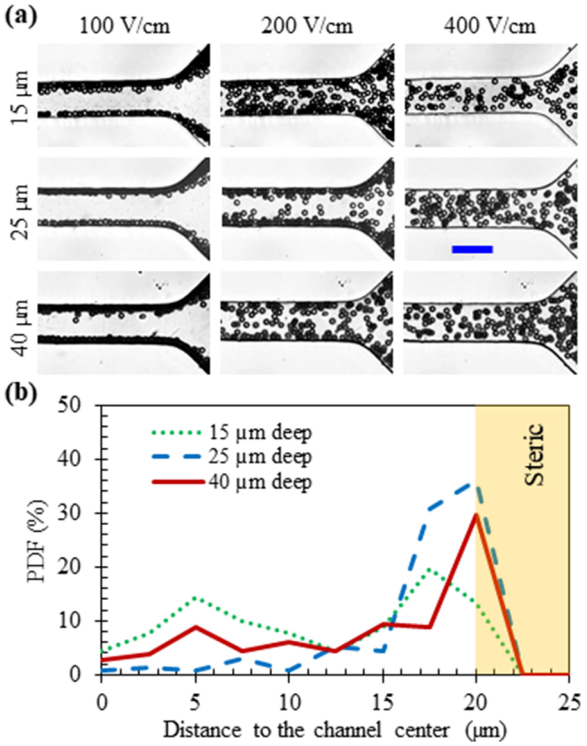

FIG. 7. Electrophoresis of 10 μm particles in 2000 ppm XG solution through microchannels of varying depths: (a) top-view superimposed images at the channel outlet under varying DC electric fields; (b) plot of particle PDF obtained from the images in (a) under the electric field of 200 V/cm. The scale bar in (a) represents 50 μm. The shaded region in (b) highlights the steric zone adjacent to any channel walls, where the center of particles cannot reach.

three depths of microchannels, i.e., 15, 25, and 40 μm, respectively. There are no visually significant differences among the top-view images in Fig. 7(a), which indicates a weak dependence of the fluid shear thinning-driven lateral migration on channel depth. This phenomenon is not surprising because the variation of channel depth has no effect on the shear rate distribution of electroosmotic flow under the thin EDL limit.[55] When the electric field is increased to 200 V/cm, more particles are observed from the images in Fig. 7(a) to migrate away from the walls at the outlet of 15 μm and 40 μm deep channels than of 25 μm deep channel. This observation is quantitatively reflected by the PDF plots in Fig. 7(b), where less than 50% of the particles are within one particle diameter from either wall of most the shallowest and deepest microchannels (as compared to 70% in 25 μm deep channel). The reason for such a non-monotonic variation of particle migration with channel depth is currently unclear. Further increasing the electric field to 400 V/cm appears to deplete particles from the walls due to the enhanced wall-repulsive electrical lift, and hence, the particle images at the outlet of any channel depths in Fig. 7(a) become visually similar again.

IV. CONCLUSIONS

We have performed an experimental study of particle electrophoresis in the DC electroosmotic flow of shear-thinning XG solutions through straight rectangular microchannels. Particles are observed to migrate towards (and eventually travel along) the channel walls at relatively low electric fields, but start moving away from the walls as the electric field increases. This observation is different from what happens in our control experiment with a Newtonian fluid, which leads us to hypothesize there are two opposing forces acting on particles in the XG solutions. The first one is a wall-induced electrical lift that directs particles towards the channel center and has been well studied in Newtonian fluids. The second force is a fluid shear thinning-induced lift that pushes particles away from the channel center. The latter migration may be heading exactly towards the four corners of the channel cross-section, which, however, requires further experimental verifications. We have also conducted a comprehensive study of the effects of various parameters of the fluid-particle-channel-(electric) field system. The fluid shear thinning-induced lift is found to increase with the XG concentration and hence the fluid shear thinning effect. It is, however, a weaker function of electric field than the electrical lift and is at most a linear function of particle size. Moreover, the channel depth does not seem to significantly affect this wall-attractive lift. We believe our presented results will be useful for future theoretical and numerical studies on particle electrophoresis in confined flows of shear thinning fluids.

ACKNOWLEDGMENTS

This work was supported in part by the NSF under Grant No. CBET-1704379 (X.X.) and by Clemson University through the Creative Inquiry Program (X.X.).

REFERENCES

[1]J. Sibbitts, K. A. Sellens, S. Jia, S. A. Klasner, and C. T. Culbertson, "Cellular analysis using microfluidics," Anal. Chem. **90**, 65–85 (2018).
[2]T. W. Murphy, Q. Zhang, L. B. Naler, S. Ma, and C. Lu, "Recent advances in the use of microfluidic technologies for single cell analysis," Analyst **143**, 60–80 (2018).
[3]X. Xuan, J. Zhu, and C. Church, "Particle focusing in microfluidic devices," Microfluid. Nanofluid. **9**, 1–16 (2010).
[4]L. Huang, S. Bian, Y. Cheng, G. Shi, P. Liu, X. Ye, and W. Wang, "Microfluidics cell sample preparation for analysis: Advances in efficient cell enrichment and precise single cell capture," Biomicrofluidics **11**, 011501 (2017).
[5]J. Nilsson, M. Evander, B. Hammarstrom, and T. Laurell, "Review of cell and particle trapping in microfluidic systems," Anal. Chim. Acta **649**, 141–157 (2009).
[6]Z. Wu, Y. Chen, M. Wang, and A. J. Chung, "Continuous inertial microparticle and blood cell separation in straight channels with local microstructures," Lab Chip **16**, 532–542 (2016).
[7]W. Connacher, N. Zhang, A. Huang, J. Mei, S. Zhang, T. Gopesh, and J. Friend, "Micro/nano acoustofluidics: Materials, phenomena, design, devices, and applications," Lab Chip **18**, 1952–1996 (2018).
[8]A. Munaz, M. J. A. Shiddiky, and N. T. Nguyen, "Recent advances and current challenges in magnetophoresis based micro magnetofluidics," Biomicrofluidics **12**, 031501 (2018).
[9]H. Yang and M. A. M. Gijs, "Micro-optics for microfluidic analytical applications," Chem. Soc. Rev. **47**, 1391–1458 (2018).
[10]C. Liu and G. Hu, "High-throughput particle manipulation based on hydrodynamic effects in microchannels," Micromachines **8**, 73 (2017).
[11]G. Yossifon, I. Frankel, and T. Miloh, "On electro-osmotic flows through micro-channel junctions," Phys. Fluids **18**, 117108 (2006).
[12]M. Zehavi and G. Yossifon, "Particle dynamics and rapid trapping in electro-osmotic flow around a sharp microchannel corner," Phys. Fluids **26**, 082002 (2014).
[13]R. A. Prabhakaran, Y. Zhou, C. Zhao, G. Hu, Y. Song, J. Wang, C. Yang, and X. Xuan, "Induced charge effects on electrokinetic entry flow," Phys. Fluids **29**, 062001 (2017).
[14]E. A. Frants, G. S. Ganchenko, V. S. Shelistov, S. Amiroudine, and E. A. Demekhin, "Nonequilibrium electrophoresis of an ion-selective microgranule for weak and moderate external electric fields," Phys. Fluids **30**, 022001 (2018).
[15]Y. Ren, W. Liu, Z. Wang, and Y. Tao, "Induced-charge electrokinetics in rotating electric fields: A linear asymptotic analysis," Phys. Fluids **30**, 062006 (2018).
[16]S. Bhattacharyya and P. S. Majee, "Nonlinear electrophoresis of a charged polarizable liquid droplet," Phys. Fluids **30**, 082008 (2018).
[17]H. C. Chang and L. Y. Yeo, *Electrokinetically-Driven Microfluidics and Nanofluidics* (Cambridge University Press, 2009).
[18]B. H. Lapizco-Encinas, B. A. Simmons, E. B. Cummings, and Y. Fintschenko, "Insulator-based dielectrophoresis for the selective concentration and separation of live bacteria in water," Electrophoresis **25**, 1695–1704 (2004).
[19]B. G. Hawkins, A. E. Smith, Y. A. Syed, and B. J. Kirby, "Continuous-flow particle separation by 3D insulative dielectrophoresis using coherently shaped, DC-biased, AC electric fields," Anal. Chem. **79**, 7291–7300 (2007).
[20]J. Zhu and X. Xuan, "Dielectrophoretic focusing of particles in a microchannel constriction using DC-biased AC electric fields," Electrophoresis **30**, 2668–2675 (2009).
[21]C. Church, J. Zhu, G. Wang, T. J. Tzeng, and X. Xuan, "Electrokinetic focusing and filtration of cells in a serpentine microchannel," Biomicrofluidics **3**, 044109 (2009).
[22]J. Zhu, T. J. Tzeng, and X. Xuan, "Continuous dielectrophoretic separation of particles in a spiral microchannel," Electrophoresis **31**, 1382–1388 (2010).
[23]M. Li, S. Li, W. Li, W. Wen, and G. Alici, "Continuous manipulation and separation of particles using combined obstacle- and curvature-induced direct current dielectrophoresis," Electrophoresis **34**, 952–960 (2013).

[24]M. Li, W. Li, J. Zhang, G. Alici, and W. Wen, "A review of microfabrication techniques and dielectrophoretic microdevices for particle manipulation and separation," J. Phys. D: Appl. Phys. **47**, 063001 (2014).
[25]B. H. Lapizco-Encinas, "On the recent developments of insulator-based dielectrophoresis: A review," Electrophoresis (in press).
[26]Y. Kang and D. Li, "Electrokinetic motion of particles and cells in microchannels," Microfluid. Nanofluid. **6**, 431–460 (2009).
[27]S. Qian and Y. Ai, *Electrokinetic Particle Transport in Micro/Nanofluidics: Direct Numerical Simulation Analysis* (CRC Press, 2012).
[28]H. J. Keh and J. A. Anderson, "Boundary effects on electrophoretic motion of colloidal spheres," J. Fluid Mech. **153**, 417–439 (1985).
[29]E. Yariv and H. Brenner, "The electrophoretic mobility of a closely fitting sphere in a cylindrical pore," SIAM J. Appl. Math. **64**, 423–441 (2003).
[30]J. P. Hsu, M. H. Ku, and C. Y. Kao, "Electrophoresis of a spherical particle along the axis of a cylindrical pore: Effect of electroosmotic flow," J. Colloid Interface Sci. **276**, 248–254 (2004).
[31]X. Xuan, S. Raghibizadeh, and D. Li, "Wall effects on electrophoretic motion of spherical polystyrene particles in a rectangular poly (dimethylsiloxane) microchannel," J. Colloid Interface Sci. **296**, 743–748 (2006).
[32]H. Liu, S. Qian, and H. Bau, "The effect of translocating cylindrical particles on the ionic current through a nanopore," Biophys. J. **92**, 1164–1177 (2007).
[33]E. Yariv and H. Brenner, "The electrophoretic mobility of an eccentrically positioned spherical particle in a cylindrical pore," Phys. Fluids **14**, 3354–3357 (2002).
[34]C. Ye, X. Xuan, and D. Li, "Eccentric electrophoretic motion of spherical particles in circular cylindrical microchannels," Microfluid. Nanofluid. **1**, 234–241 (2005).
[35]X. Xuan, C. Ye, and D. Li, "Near-wall electrophoretic motion of spherical particles in cylindrical capillaries," J. Colloid Interface Sci. **289**, 286–290 (2005).
[36]Q. Liang, C. Zhao, and C. Yang, "Enhancement of electrophoretic mobility of microparticles near a solid wall: Experimental verification," Electrophoresis **36**, 731–736 (2015).
[37]L. Liang, Y. Ai, J. Zhu, S. Qian, and X. Xuan, "Wall-induced lateral migration in particle electrophoresis through a rectangular microchannel," J. Colloid Interface Sci. **347**, 142–146 (2010).
[38]Z. Liu, D. Li, Y. Song, X. Pan, D. Li, and X. Xuan, "Surface-conduction enhanced dielectrophoretic-like particle migration in electric-field driven fluid flow through a straight rectangular microchannel," Phys. Fluids **29**, 102001 (2017).
[39]E. Yariv, "Force-free electrophoresis?," Phys. Fluids **18**, 031702 (2006).
[40]H. Zhao and H. Bau, "On the effect of induced electro-osmosis on a cylindrical particle next to a surface," Langmuir **23**, 4053–4063 (2007).
[41]M. Yoda and Y. Kazoe, "Dynamics of suspended colloidal particles near a wall: Implications for interfacial particle velocimetry," Phys. Fluids **23**, 111301 (2011).
[42]E. Yariv, "Dielectrophoretic sphere–wall repulsion due to a uniform electric field," Soft Matter **12**, 6277–6284 (2016).
[43]Y. W. Kim and J. Y. Yoo, "Axisymmetric flow focusing of particles in a single microchannel," Lab Chip **9**, 1043–1045 (2009).
[44]N. Cevheri and M. Yoda, "Lift forces on colloidal particles in combined electroosmotic and Poiseuille flow," Langmuir **30**, 13771–13780 (2014).
[45]D. Yuan, C. Pan, J. Zhang, S. Yan, Q. Zhao, G. Alici, and W. Li, "Tunable particle focusing in a straight channel with symmetric semicircle obstacle arrays using electrophoresis-modified inertial effects," Micromachines **7**, 195 (2016).
[46]N. Cevheri and M. Yoda, "Electrokinetically driven reversible banding of colloidal particles near the wall," Lab Chip **14**, 1391 (2014).
[47]A. Yee and M. Yoda, "Experimental observations of bands of suspended colloidal particles subject to shear flow and steady electric field," Microfluid. Nanofluid. **22**, 113 (2018).
[48]G. D'Avino, G. Greco, and P. L. Maffettone, "Particle migration due to viscoelasticity of the suspending liquid and its relevance in microfluidic devices," Annu. Rev. Fluid. Mech. **49**, 341–360 (2017).
[49]X. Lu, C. Liu, G. Hu, and X. Xuan, "Particle manipulations in non-Newtonian microfluidics: A review," J. Colloid Interface Sci. **500**, 182–201 (2017).
[50]J. J. Sousa, A. M. Afonso, F. T. Pinho, and M. A. Alves, "Effect of the skimming layer on electro-osmotic–Poiseuille flows of viscoelastic fluids," Microfluid. Nanofluid. **10**, 107–122 (2011).
[51]C. Zhao and C. Yang, "Electroosmotic flows of non-Newtonian power-law fluids in a cylindrical microchannel," Electrophoresis **34**, 662–667 (2013).
[52]S. Chen, X. He, V. Bertola, and M. Wang, "Electro-osmosis of non-Newtonian fluids in porous media using lattice Poisson–Boltzmann method," J. Colloid Interface Sci. **436**, 186–193 (2014).
[53]X. Guo and H. Qi, "Analytical solution of electro-osmotic peristalsis of fractional Jeffreys fluid in a micro-channel," Micromachines **8**, 341 (2017).
[54]L. Mei, H. Zhang, H. Meng, and S. Qian, "Electroosmotic flow of viscoelastic fluid in a nanoslit," Micromachines **9**, 155 (2018).
[55]C. Zhao and C. Yang, "Electrokinetics of non-Newtonian fluids: A review," Adv. Colloid Interface Sci. **201-202**, 94–108 (2013).
[56]E. Lee, Y. F. Huang, and J. P. Hsu, "Electrophoresis in a non-Newtonian fluid: Sphere in a spherical cavity," J. Colloid Interface Sci. **258**, 283–288 (2003).
[57]E. Lee, C. T. Chen, and J. P. Hsu, "Electrophoresis of a rigid sphere in a Carreau fluid normal to a planar surface," J. Colloid Interface Sci. **285**, 857–864 (2005).
[58]J. P. Hsu and L. H. Yeh, "Effect of a charged boundary on electrophoresis in a Carreau fluid: A sphere at an arbitrary position in a spherical cavity," Langmuir **23**, 8637–8646 (2007).
[59]L. H. Yeh and J. P. Hsu, "Electrophoresis of a finite rod along the axis of a long cylindrical microchannel filled with Carreau fluids," Microfluid. Nanofluid. **7**, 383–392 (2009).
[60]A. S. Khair, D. E. Posluszny, and L. M. Walker, "Coupling electrokinetics and rheology: Electrophoresis in non-Newtonian fluids," Phys. Rev. E **85**, 016320 (2012).
[61]R. M. Bryce and M. R. Freeman, "Extensional instability in electro-osmotic microflows of polymer solutions," Phys. Rev. E **81**, 036328 (2010).
[62]F. Pimenta and M. A. Alves, "Electro-elastic instabilities in cross-shaped microchannels," J. Non-Newtonian Fluid Mech. **259**, 61–77 (2018).
[63]C. H. Ko, D. Li, A. Malekanfard, Y. N. Wang, L. M. Fu, and X. Xuan, "Electroosmotic flow of non-Newtonian fluids in a constriction microchannel," Electrophoresis (in press).
[64]A. Lindner, D. Bonn, and J. Meunier, "Viscous fingering in a shear-thinning fluid," Phys. Fluids **12**, 256–261 (2000).
[65]P. E. Arratia, G. A. Voth, and J. P. Gollub, "Stretching and mixing of non-Newtonian fluids in time-periodic flows," Phys. Fluids **17**, 053102 (2005).
[66]X. Lu, S. Patel, M. Zhang, S. Joo, S. Qian, A. Ogale, and X. Xuan, "An unexpected particle oscillation for electrophoresis in viscoelastic fluids through a microchannel constriction," Biomicrofluidics **8**, 021802 (2014).
[67]X. Lu, J. DuBose, S. Qian, S. Joo, and X. Xuan, "Viscoelastic effects on electrokinetic particle focusing in a constricted microchannel," Biomicrofluidics **9**, 014108 (2015).
[68]D. Li and X. Xuan, "Electrophoretic slip-tuned particle migration in microchannel viscoelastic fluid flows," Phys. Rev. Fluids **3**, 074202 (2018).
[69]L. Liang, S. Qian, and X. Xuan, "Three-dimensional electrokinetic particle focusing in a rectangular microchannel," J. Colloid Interface Sci. **350**, 377–379 (2010).
[70]A. Japper-Jaafar, M. P. Escudier, and R. J. Poole, "Laminar, transitional and turbulent annular flow of drag-reducing polymer solutions," J. Non-Newtonian Fluid Mech. **165**, 1357–1372 (2010).

[71] X. Xuan, "Joule heating in electrokinetic flow," Electrophoresis **29**, 33–43 (2008).
[72] D. Yan, C. Yang, and X. Huang, "Effect of finite reservoir size on electroosmotic flow in microchannels," Microfluid. Nanofluid. **3**, 333–340 (2007).
[73] R. B. Bird, R. C. Armstrong, and O. Hassager, *Dynamics of Polymeric Liquids* (Wiley-Interscience, 1977), Vol. 1.
[74] H. A. Barnes, J. F. Hutton, and K. Walters, *An Introduction to Rheology* (Elsevier, Amsterdam, 1989).